2D Raman imaging for rotational and vibrational temperature mapping

D. Del Cont-Bernard, M.D. Ruijzendaal, T.W.H. Righart, G.J. van Rooij, T.D. Butterworth
Department of Circular Chemical Engineering, Faculty of Science and Engineering, Maastricht University, PO Box 616, 6200 MD, Maastricht, The Netherlands

Abstract: 2D rovibrational temperature imaging is developed for H_2 Raman features. Images are collected with an ICCD camera fitted with different bandpass filters, each selecting well separated spectral features of the H_2 rotational and vibrational Raman spectrum. A pixel-based discrete spectrum is obtained from the multispectral images from which temperatures are determined with pre-calculated calibration curves. Regular 0D and 1D measurements validate the method.

Keywords: 2D Raman scattering, Hydrogen plasmas, Bandpass filters, Thermometry

1. Introduction

Hydrogen plays a significant role in various plasma processes of industrial significance, including semiconductor production, methane reforming, and hydrocarbon processing. As hydrogen continues to gain recognition as an energy carrier, its applications can be expected to increase, with hydrogen and ammonia combustion receiving more attention. Temperature is a crucial parameter in both plasma processes and combustion applications; temperature control is necessary for tuning reaction conditions and understanding the behaviour of reactors. The analysis of spontaneous Raman scattering is known to be a reliable method for accurately measuring temperature. However, if a spectrometer is used in the analysis of the Raman scattering, only point or line measurements are possible because one dimension of the camera sensor is used to separate the signal according to wavelength.

In this work, we propose the use of multiple filters and the collection of multispectral images for temperatures determination. This approach has been shown to be effective for hydrogen due to the unique properties of its rotational Raman spectrum. In [B1], 2D temperature and hydrogen concentration imaging were performed in a hydrogen jet expanding in a nitrogen background. Building upon that work, we extend it to the case of reactive flows and a much larger temperature range. Most importantly, in this work, we pave the way for measurements of 2D non-equilibrium in hydrogen-containing plasmas by measuring both the vibrational and rotational temperature.

2. Method

The rotational Raman spectrum of hydrogen features peaks that are very well spaced in the wavelength axis, owing to its large rotational constant, B. In case of an excitation wavelength of 532 nm, the rotational Raman spectrum spans several tens of nm, enabling the use of narrowband (10 nm) bandpass filters to even perfectly isolate peaks from molecules with different rotational quantum numbers, J.

Figure 1 compares the simulated rotational Raman spectrum with the transmission window of some selected commercial filters.

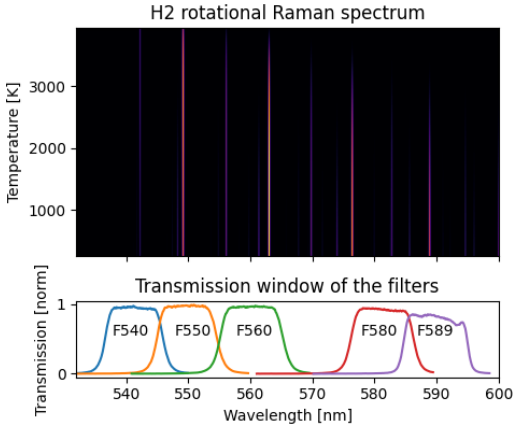

Fig. 1. Simulated rotational Raman spectrum of H2, compared with the transmission window of a few commercially available narrowband bandpass filters.

In the 2D imaging mode, filters are used to obtain multispectral images. Each pixel of the multispectral image has multiple channels, effectively describing a discrete spectrum, from which, the temperature can be determined using a pre-calculated curve. To enhance the acquisition of the weak Raman signal, 4x4 or 8x8 on-chip binning is applied. A background image without laser light is also acquired to eliminate any in-band interference.

Based on simulations of the H_2 Raman spectrum and filters transmission curves, the signal strength for each filter can be predicted for a given temperature. A calibration curve (Fig. 2) relating signal intensities and temperature can be constructed by normalizing the amplitude of all channels to one. A required assumption is that the population of the different rotational levels follows a Boltzmann distribution. The temperature is estimated by finding the closest point on the calibration curve to the normalized experimental data.

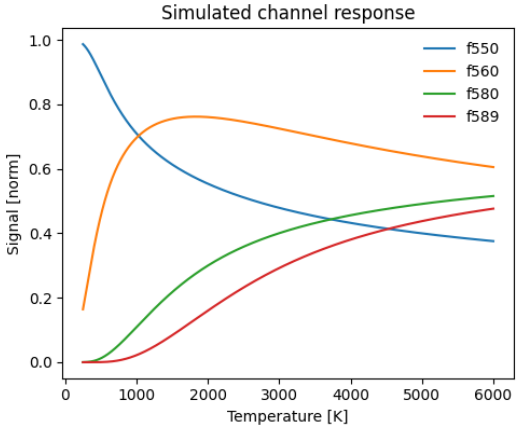

Fig. 2. The calibration curve used to determine rotational temperature, showing for each temperature the expected (normalized) signal collected with different filters.

The vibrational temperature is determined by the ratio between the vibrational Raman Stokes and anti-Stokes signal intensity, also using a pre-calculated calibration curve, similarly as in [T1]. Given that the two regions of interest are far apart in wavelength, transmission properties of all optics and quantum efficiency of the camera become important. In this preliminary work we did not perform and radiometric calibration, but it will be required to correctly determine the vibrational temperature.

For the 1D temperature measurements, a spectrometer is used. In these cases, the region of interest can be scanned by translating the system (i.e., plasma) under study relative to the laser. The temperature determination is performed by fitting a simulated spectrum to the experimental one. When considering the rotational Raman spectra, the vibrational temperature is assumed equal to the rotational one. When considering the rovibrational spectra, the two temperatures are fitted independently.

3. Experimental setup

In 2D imaging mode (Fig. 3b), a 532 nm laser beam from a Continuum Powerlite 9030 frequency doubled Nd:YAG laser is sent through a cylindrical lens (f=1.75 m) to form a 10 mm tall laser sheet with an energy of 0.5 J at the region of interest. The scattered light is collected by a 1" 100 mm focal length lens, passed through a polarizing filter, a filter slider with different bandpass filters, a notch filter centred at 532 nm to remove Rayleigh scattering, and finally focused onto an ICCD camera (Andor DH334T-18F-63).

In the spectrometer mode (Fig. 3a), a second cylindrical lens (f=1.75 m) is added to loosely focus the beam in both directions without inducing breakdown. The laser pulse energy must be decreased to about 0.2 J to avoid stimulated Raman. The Raman scattering is collected by a 1" 100 mm focal length lens, goes through a polarizing filter and a notch filter and it is focused onto an optical fibre bundle (19 × 200 μm fibres) that leads to a commercial Czerny-Turner spectrometer (Andor Kymera 328i). The signal is imaged with the same camera used in 2D imaging mode.

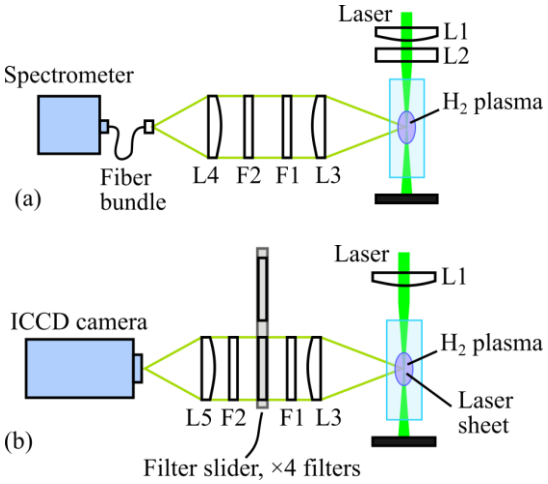

Fig. 3. Experimental setup. (a) Configuration with spectrometer (0D or 1D measurements), (b) Configuration with a camera (2D measurements). L1, L2: f=1750 mm cylindrical lens, L3, L4: spherical lens f=100 mm; L5: spherical lens f=80 mm. F1: polarizing filter; F2: notch filter at 532 nm. Filters in the slider are discussed in the text.

Four filter are used for the rotational temperature determination and have a 10 nm transmission window centred at 550, 560, 580, 589 nm. Two filters with a 50 nm transmission window centred at 425 nm and 675 nm are used for the vibrational temperature estimation.

The procedure is tested on a microwave H_2 plasma. Details of the reactor are not relevant for the purposes of this paper. The system is reminiscent of the one described for example in [D1]. The plasma is generated inside a 30 mm diameter quartz tube, featuring a swirl injector. The H_2 flowrate is 15 slpm, the absorbed microwave power about 300 W and the pressure in the reactor about 130 mbar.

4. Results

Figure 4 provides an example of raw data obtained with the four different filters used for determining the rotational temperature (F550, F560, F580, F589). Figure 5 instead shows the whole vibrational Stokes and anti-Stokes signal, to be used for the vibrational temperature estimation. Note that the signal intensity reflects not only the actual signal strength but also the different quantum efficiency of the camera and different transmission of the optics at different wavelengths. Additionally, note that the preliminary data shown in Fig. 4 and Fig 5 were collected in different days, when both the plasma and the optics alignment could have been slightly different.

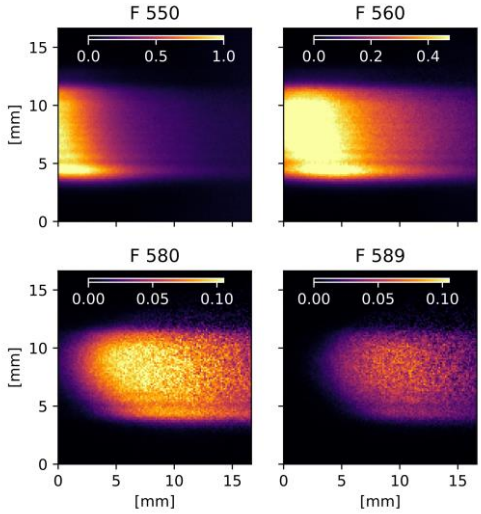

Fig. 4. Examples of the rotational Raman signal captured with different filters. The centre wavelength in nm of the used filter is reported on the title of each panel.

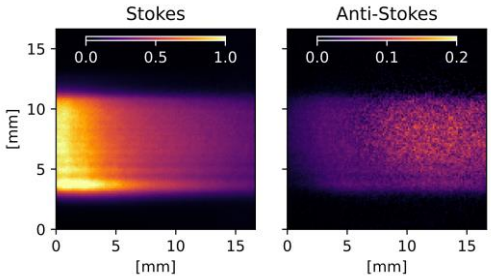

Fig. 5. Examples of the vibration Stokes and anti-Stokes signal collected using the two bandpass filters at 450 and 675 nm.

Following the procedure described above, the rotational temperature could be calculated from the data of Fig. 4, and the result is shown in Fig. 6. Rotational temperatures spanning from 300 K up to about 2500 K are observed. Interestingly, the plasma emission appears only in a small region compared to the overall high-temperature region. The false colour plasma image is obtained by using as RGB channels the plasma luminescence recorded with three different bandpass filters.

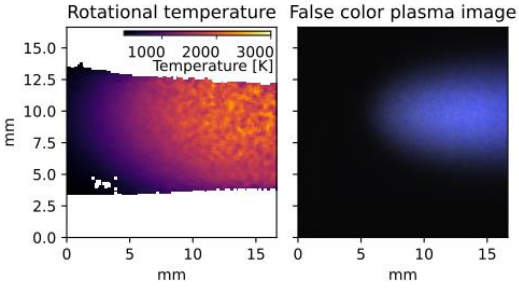

Fig. 6. Sample results of the estimated rotational temperature, compared with a false colour image of the plasma emission.

Figure 7 shows a preliminary evaluation of the vibrational anti-Stokes / Stokes ratio, that can be used to determine ν_1/ν_0 vibrational temperature. The calibration of this is in progress. Based on the raw data, the S/AS ratio map reveals a hot plasma core with cold edges, similar to figure 6. In the presentation, the 2D vibrational temperature map will be compared with the rotational temperature one.

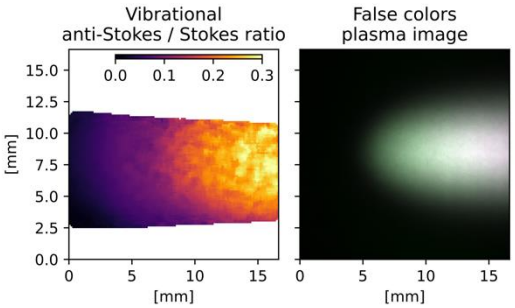

Fig. 7. Sample results of the vibration anti-Stokes / Stokes ratio, compared with a false colour image of the plasma emission.

Finally, Figure 8 compares temperature estimations obtained along the centreline of the reactor using either a spectrometer or the camera and filters. The temperature discrepancies in Fig. 8 can be partially explained by variations in plasma conditions and alignment, as the data were collected on different days. A more consistent set of data will be produced for the presentation.

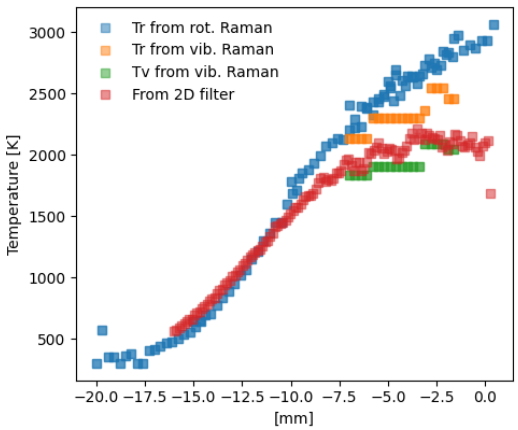

Fig. 8. Preliminary comparison of the temperature estimations along the centreline produced using different methods. The first 3 datasets were obtained using the spectrometer by scanning the region of interest. Blue datapoints are estimations of the rotational temperature (T_r) obtained fitting the rotational Raman spectrum. The orange and green points are instead the estimated rotational (T_r) and vibrational temperatures (T_v) respectively, obtained by

fitting the vibrational spectrum of H_2. The latter dataset, in red, is instead extracted from the 2D data shown in Fig. 6.

5. Discussion

We have demonstrated an accurate method for 2D imaging of rotational and vibrational temperature from the H_2 Raman spectrum. One of the benefits of this method is that it can significantly speed up Raman data-acquisition, particularly if a high pulse-energy laser is available. One of the limiting factors in 0D and 1D Raman spectrum acquisition is the onset of laser induced breakdown and non-linear optical effects at high laser fluences. These limitations effectively impose a maximum Raman signal acquisition rate per sample area. By using laser sheets, the same laser fluence limitations apply, but much higher laser pulse energies can be used. This effectively means the laser energy is dispersed over a larger volume but with identical laser fluence, and so the same Raman signal rate per area can be achieved.

However, this benefit in acquisition speed comes with a disadvantage – namely that information is lost. Raman spectra contain information on rotational and vibrational population distributions, whilst 2D imaging Raman loses this information, especially for the vibrational modes. Consequently, non-Boltzmann distributions of vibrational energy would be overlooked in the imaging mode.

There are also some challenges to implementing this technique in a robust manner, and care should be taken in the set-up of the experiment and data analysis. Two main challenges have been identified:

The first one relates with a pixel-dependent filter behaviour. When doing 2D imaging, the collimated signal, in general, does not arrive at normal incidence angle at the filters. For an interference filter, the angle of incidence of the light strongly determines the centre wavelength of the transmission window. The result is that the light focused on different pixels has gone through different effective filters. This issue can be addressed in post-processing using pixel-based calibration curves, or by using a low numerical aperture in the signal collection.

The second challenge involves the presence of interfering signals. The method can be applied to plasmas and flames containing H2, but only in cases where there is no strong background in the transmission window for the chosen filters. Plasmas containing hydrocarbons pose an interesting case. According to the pressure and the temperature profiles inside the reactor, C_2 radicals could be generated and C_2 laser induced fluorescence (LIF) could become the dominant emission in the region where the rotational Raman signal of H_2 is expected. Disentangling the laser-induced background from the signal is a significant challenge. Previous works [T1] suggest exploiting the polarization properties of the Raman signal, as the LIF signal is not polarized. Exploring different excitation wavelength could also provide an alternative route to avoid LIF [T2].

6. Conclusions

In this abstract, we have demonstrated a method for 2D imaging of H_2 rotational and vibrational temperatures. The 2D rotational temperature estimations are compared with 1D measurements obtained from fitting a detailed Raman spectrum. The vibrational temperature calculations are ongoing, but examples of uncalibrated vibrational Stokes/anti-Stokes ratios are provided. During the presentation, a consistent set of measurements will be presented, and a thorough validation will be offered.

7. References

[B1] Braeuer, Andreas, and Alfred Leipertz. "Two-dimensional Raman mole-fraction and temperature measurements for hydrogen-nitrogen mixture analysis." *Applied optics* 48.4 (2009): B57-B64.

[P1] Van de Steeg, A. W., et al. "Plasma activation of N2, CH4 and CO2: an assessment of the vibrational non-equilibrium time window." Plasma Sources Science and Technology 29.11 (2020): 115001.

[D1] Bongers, Waldo, et al. "Plasma-driven dissociation of CO2 for fuel synthesis." Plasma processes and polymers 14.6 (2017): 1600126.

[T1] Rabenstein, Friedrich, and Alfred Leipertz. "Two-dimensional temperature determination in the exhaust region of a laminar flat-flame burner with linear Raman scattering." Applied Optics 36.27 (1997): 6989-6996.

[T2] Rabenstein, Friedrich, and Alfred Leipertz. "One-dimensional, time-resolved Raman measurements in a sooting flame made with 355-nm excitation." Applied optics 37.21 (1998): 4937-4943.